Hindawi Publishing Corporation
EURASIP Journal on Audio, Speech, and Music Processing
Volume 2007, Article ID 84376, 8 pages
doi:10.1155/2007/84376

Research Article

A Low Delay and Fast Converging Improved Proportionate Algorithm for Sparse System Identification

Andy W. H. Khong,[1] Patrick A. Naylor,[1] and Jacob Benesty[2]

[1] *Department of Electrical and Electronic Engineering, Imperial College London, Exhibition Road, London SW7 2AZ, UK*
[2] *INRS-EMT, Université du Québec, Suite 6900, 800 de la Gauchetière Ouest, Montréal, QC, Canada H5A 1K6*

Received 4 July 2006; Revised 1 December 2006; Accepted 24 January 2007

Recommended by Kutluyil Dogancay

A sparse system identification algorithm for network echo cancellation is presented. This new approach exploits both the fast convergence of the improved proportionate normalized least mean square (IPNLMS) algorithm and the efficient implementation of the multidelay adaptive filtering (MDF) algorithm inheriting the beneficial properties of both. The proposed IPMDF algorithm is evaluated using impulse responses with various degrees of sparseness. Simulation results are also presented for both speech and white Gaussian noise input sequences. It has been shown that the IPMDF algorithm outperforms the MDF and IPNLMS algorithms for both sparse and dispersive echo path impulse responses. Computational complexity of the proposed algorithm is also discussed.

1. INTRODUCTION

Research on network echo cancellation is increasingly important with the advent of voice over internet protocol (VoIP). In such systems where traditional telephony equipment is connected to the packet-switched network, the echo path impulse response, which is typically of length 64–128 milliseconds, exhibits an "active" region in the range of 8–12 milliseconds duration and consequently, the impulse response is dominated by regions where magnitudes are close to zero making the impulse response sparse. The "inactive" region is due to the presence of bulk delay caused by network propagation, encoding, and jitter buffer delays [1]. Other applications for sparse system identification include wavelet identification using marine seismic signals [2] and geophysical seismic applications [3, 4].

Classical adaptive algorithms with a uniform step-size across all filter coefficients such as the normalized least mean square (NLMS) algorithm have slow convergence in sparse network echo cancellation applications. One of the first algorithms which exploits the sparse nature of network impulse responses is the proportionate normalized least mean square (PNLMS) algorithm [5] where each filter coefficient is updated with an independent step-size which is proportional to the estimated filter coefficient. Subsequent improved versions such as the IPNLMS [6] and IIPNLMS [7] algorithms were proposed, which achieve improved convergence by introducing a controlled mixture of proportionate (PNLMS) and nonproportionate (NLMS) adaptation. Consequently, these algorithms perform better than PNLMS for sparse and, in some cases, for dispersive impulse responses. To reduce the computational complexity of PNLMS, the sparse partial update NLMS (SPNLMS) algorithm was proposed [8] where, similar to the selective partial update NLMS (SPUNLMS) algorithm [9], only taps corresponding to the M largest absolute values of the product of input signal and filter coefficients are selected for adaptation. An optimal step-size for PNLMS has been derived in [10] and employing an approximate μ-law function, the proposed segment PNLMS (SPNLMS) outperforms the PNLMS algorithm.

In recent years, frequency-domain adaptive algorithms have become popular due to their efficient implementation. These algorithms incorporate block updating strategies whereby the fast Fourier transform (FFT) algorithm [11] is used together with the overlap-save method [12, 13]. One of the main drawbacks of these approaches is the delay introduced between the input and output which can be equivalent to the length of the adaptive filter. Consequently, for long impulse responses, this delay can be considerable since the number of filter coefficients can be several thousands [14]. To

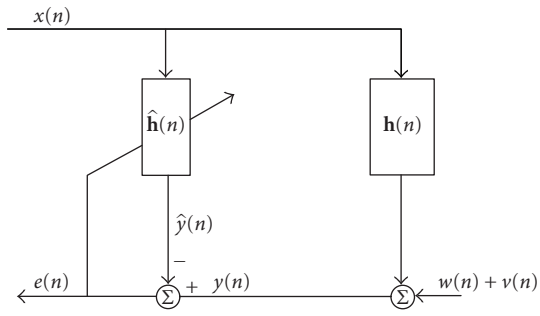

Figure 1: Schematic diagram of an echo canceller.

mitigate this problem, Soo and Pang proposed the multidelay filtering (MDF) algorithm [15] which uses a block length N independent of the filter length L. Although it has been well-known, from the computational complexity point of view, that $N = L$ is the optimal choice, the MDF algorithm nevertheless is more efficient than time-domain implementations even for $N < L$ [16].

In this paper, we propose and evaluate the improved proportionate multidelay filtering (IPMDF) algorithm for sparse impulse responses.[1] The IPMDF algorithm exploits both the improvement in convergence brought about by the proportionality control of the IPNLMS algorithm and the efficient implementation of the MDF structure. As will be explained, direct extension of the IPNLMS algorithm to the MDF structure is inappropriate due to the dimension mismatch between the update vectors. Consequently, in contrast to the MDF structure, adaptation for the IPMDF algorithm is performed in the time domain. We then evaluate the performance of IPMDF using impulse responses with various degrees of sparseness [18, 19]. This paper is organized as follows. In Section 2, we review the PNLMS, IPNLMS, and MDF algorithms. We then derive the proposed IPMDF algorithm in Section 3 while Section 3.2 presents the computational complexity. Section 4 shows simulation results and Section 5 concludes our work.

2. ADAPTIVE ALGORITHMS FOR SPARSE SYSTEM IDENTIFICATION

With reference to Figure 1, we first define filter coefficients and tap-input vector as

$$\begin{aligned}\hat{\mathbf{h}}(n) &= \left[\hat{h}_0(n), \hat{h}_1(n), \ldots, \hat{h}_{L-1}(n)\right]^T,\\ \mathbf{x}(n) &= \left[x(n), x(n-1), \ldots, x(n-L+1)\right]^T,\end{aligned} \tag{1}$$

where L is the adaptive filter length and the superscript T is defined as the transposition operator. The adaptive filter will model the unknown impulse response $\mathbf{h}(n)$ using the near-end signal

$$y(n) = \mathbf{x}^T(n)\mathbf{h}(n) + v(n) + w(n), \tag{2}$$

where $v(n)$ and $w(n)$ are defined as the near-end speech signal and ambient noise, respectively. For simplicity, we will temporarily ignore the effects of double talk and ambient noise, that is, $v(n) = w(n) = 0$, in the description of algorithms.

2.1. The PNLMS and IPNLMS algorithms

The proportionate normalized least mean square (PNLMS) [5] and improved proportionate normalized least mean square (IPNLMS) [6] algorithms have been proposed for network echo cancellation where the impulse response of the system is sparse. These algorithms can be generalized using the following set of equations:

$$e(n) = y(n) - \hat{\mathbf{h}}^T(n-1)\mathbf{x}(n), \tag{3}$$

$$\hat{\mathbf{h}}(n) = \hat{\mathbf{h}}(n-1) + \frac{\mu\mathbf{Q}(n-1)\mathbf{x}(n)e(n)}{\mathbf{x}^T(n)\mathbf{Q}(n-1)\mathbf{x}(n) + \delta}, \tag{4}$$

$$\mathbf{Q}(n-1) = \operatorname{diag}\left\{q_0(n-1), \ldots, q_{L-1}(n-1)\right\}, \tag{5}$$

where μ is the adaptive step-size and δ is the regularization parameter. The $L \times L$ diagonal control matrix $\mathbf{Q}(n)$ determines the step-size of each filter coefficient and is dependent on the specific algorithm as described below.

2.1.1. PNLMS

The PNLMS algorithm assigns higher step-sizes for coefficients with higher magnitude using a control matrix $\mathbf{Q}(n)$. Elements of the control matrix for PNLMS can be expressed as [5]

$$\begin{aligned}q_l(n) &= \frac{\kappa_l(n)}{\sum_{i=0}^{L-1}\kappa_i(n)},\\ \kappa_l(n) &= \max\left\{\rho \times \max\left\{\gamma, \left|\hat{h}_0(n)\right|, \ldots, \left|\hat{h}_{L-1}(n)\right|\right\}, \left|\hat{h}_l(n)\right|\right\}\end{aligned} \tag{6}$$

with $l = 0, 1, \ldots, L-1$ being the tap-indices. The parameter γ, with a typical value of 0.01, prevents $\hat{h}_l(n)$ from stalling during initialization stage where $\hat{\mathbf{h}}(0) = \mathbf{0}_{L\times 1}$ while ρ prevents coefficients from stalling when they are much smaller than the largest coefficient. The regularization parameter δ in (4) for PNLMS should be taken as

$$\delta_{\text{PNLMS}} = \frac{\delta_{\text{NLMS}}}{L}, \tag{7}$$

where $\delta_{\text{NLMS}} = \sigma_x^2$ is the variance of the input signal [6]. It can be seen that for $\rho \geq 1$, PNLMS is equivalent to NLMS.

[1] An earlier version of this work was presented at the EUSIPCO 2005 special session on sparse and partial update adaptive filters [17].

2.1.2. IPNLMS

An enhancement of PNLMS is the IPNLMS algorithm [6] which is a combination of PNLMS and NLMS with the relative significance of each controlled by a factor α. The elements of the control matrix $\mathbf{Q}(n)$ for IPNLMS are given by

$$q_l(n) = \frac{1-\alpha}{2L} + (1+\alpha)\frac{|\hat{h}_l(n)|}{2\|\hat{\mathbf{h}}\|_1 + \epsilon}, \tag{8}$$

where ϵ is a small value and $\|\cdot\|_1$ is the l_1-norm operator. It can be seen from the second term of (8) that the magnitude of the estimated taps is normalized by the l_1 norm of $\hat{\mathbf{h}}$. This shows that the weighting on the step-size for IPNLMS is dependent only on the relative scaling of the filter coefficients as opposed to their absolute values. Results presented in [6, 17] have shown that good choices of α values are 0, -0.5, and -0.75. The regularization parameter δ in (4) for IPNLMS should be taken [6] as

$$\delta_{\text{IPNLMS}} = \frac{1-\alpha}{2L}\delta_{\text{NLMS}}. \tag{9}$$

This choice of regularization ensures that the IPNLMS algorithm achieves the same asymptotic steady-state normalized misalignment compared to that of the NLMS algorithm. It can be seen that IPNLMS is equivalent to NLMS when $\alpha = -1$ while, for α close to 1, IPNLMS behaves like PNLMS.

2.2. The frequency-domain MDF algorithm

Frequency-domain adaptive filtering has been introduced as a form of improving the efficiency of time-domain algorithms. Although substantial computational savings can be achieved, one of the main drawbacks of frequency-domain approaches is the inherent delay introduced [13]. The multidelay filtering (MDF) algorithm [15] was proposed to mitigate the delay problem by partitioning the adaptive filter into K blocks each having length N such that $L = KN$. The MDF algorithm can be summarized by first letting m be the frame index and defining the following quantities:

$$\mathbf{x}(mN) = \left[x(mN), \ldots, x(mN - L + 1)\right]^T, \tag{10}$$

$$\mathbf{X}(m) = \left[\mathbf{x}(mN), \ldots, \mathbf{x}(mN + N - 1)\right], \tag{11}$$

$$\mathbf{y}(m) = \left[y(mN), \ldots, y(mN + N - 1)\right]^T, \tag{12}$$

$$\hat{\mathbf{y}}(m) = \left[\hat{y}(mN), \ldots, \hat{y}(mN + N - 1)\right]^T = \mathbf{X}^T(m)\hat{\mathbf{h}}(m), \tag{13}$$

$$\mathbf{e}(m) = \mathbf{y}(m) - \hat{\mathbf{y}}(m) = \left[e(mN), \ldots, e(mN + N - 1)\right]^T. \tag{14}$$

We note that $\mathbf{X}(m)$ is a Toeplitz matrix of dimension $L \times N$. Defining k as the block index and $\mathbf{T}(m-k)$ as an $N \times N$ Toeplitz matrix such that

$$\mathbf{T}(m-k) = \begin{bmatrix} x(mN-kN) & \cdots & x(mN-kN-N+1) \\ x(mN-kN+1) & \ddots & \vdots \\ \vdots & \ddots & \vdots \\ x(mN-kN+N-1) & \cdots & x(mN-kN) \end{bmatrix}, \tag{15}$$

it can be shown using (13) and (15) that the adaptive filter output can be expressed as

$$\hat{\mathbf{y}}(m) = \sum_{k=0}^{K-1} \mathbf{T}(m-k)\hat{\mathbf{h}}_k(m), \tag{16}$$

where

$$\hat{\mathbf{h}}_k(m) = \left[\hat{h}_{kN}(m), \hat{h}_{kN+1}(m), \ldots, \hat{h}_{kN+N-1}(m)\right]^T \tag{17}$$

is the kth subfilter of $\hat{\mathbf{h}}(m)$ for $k = 0, 1, \ldots, K-1$.

It can be shown that the Toeplitz matrix $\mathbf{T}(m-k)$ can be transformed, by doubling its size, to a circulant matrix

$$\mathbf{C}(m-k) = \begin{bmatrix} \mathbf{T}'(m-k) & \mathbf{T}(m-k) \\ \mathbf{T}(m-k) & \mathbf{T}'(m-k) \end{bmatrix} \tag{18}$$

with

$$\mathbf{T}'(m-k) = \begin{bmatrix} x(mN-kN+N) & \cdots & x(mN-kN+1) \\ x(mN-kN-N+1) & \ddots & \vdots \\ \vdots & \ddots & \vdots \\ x(mN-kN-1) & \cdots & x(mN-kN+N) \end{bmatrix}. \tag{19}$$

The resultant circulant matrix $\mathbf{C}$ can then be decomposed [20] as

$$\mathbf{C} = \mathbf{F}^{-1}\mathbf{D}\mathbf{F}, \tag{20}$$

where $\mathbf{F}$ is a $2N \times 2N$ Fourier matrix and $\mathbf{D}$ is a diagonal matrix whose elements are the discrete Fourier transform of the first column of $\mathbf{C}$. Note that the diagonal of $\mathbf{T}'$ is arbitrary, but it is normally equal to the first sample of the previous block $k-1$ [16]. We now define the frequency-domain quantities:

$$\begin{aligned} \underline{\mathbf{y}}(m) &= \mathbf{F}\begin{bmatrix} \mathbf{0}_{N\times 1} \\ \mathbf{y}(m) \end{bmatrix}, \qquad \underline{\hat{\mathbf{h}}}_k(m) = \mathbf{F}\begin{bmatrix} \hat{\mathbf{h}}_k(m) \\ \mathbf{0}_{N\times 1} \end{bmatrix}, \\ \underline{\mathbf{e}}(m) &= \mathbf{F}\begin{bmatrix} \mathbf{0}_{N\times 1} \\ \mathbf{e}(m) \end{bmatrix}, \qquad \mathbf{G}^{01} = \mathbf{F}\mathbf{W}^{01}\mathbf{F}^{-1}, \\ \mathbf{W}^{01} &= \begin{bmatrix} \mathbf{0}_{N\times N} & \mathbf{0}_{N\times N} \\ \mathbf{0}_{N\times N} & \mathbf{I}_{N\times N} \end{bmatrix}, \qquad \mathbf{G}^{10} = \mathbf{F}\mathbf{W}^{10}\mathbf{F}^{-1}, \\ \mathbf{W}^{10} &= \begin{bmatrix} \mathbf{I}_{N\times N} & \mathbf{0}_{N\times N} \\ \mathbf{0}_{N\times N} & \mathbf{0}_{N\times N} \end{bmatrix}. \end{aligned} \tag{21}$$

The MDF adaptive algorithm is then given by the following equations:

$$\underline{\mathbf{e}}(m) = \underline{\mathbf{y}}(m) - \mathbf{G}^{01} \times \sum_{k=0}^{K-1} \mathbf{D}(m-k)\underline{\hat{\mathbf{h}}}_k(m-1), \tag{22}$$

$$\mathbf{S}_{\mathrm{MDF}}(m) = \lambda \mathbf{S}_{\mathrm{MDF}}(m-1) + (1-\lambda)\mathbf{D}^*(m)\mathbf{D}(m), \tag{23}$$

$$\begin{aligned}\underline{\hat{\mathbf{h}}}_k(m) = \underline{\hat{\mathbf{h}}}_k(m-1) &+ \mu \mathbf{G}^{10}\mathbf{D}^*(m-k) \\ &\times \left[\mathbf{S}_{\mathrm{MDF}}(m) + \delta_{\mathrm{MDF}}\right]^{-1}\underline{\mathbf{e}}(m),\end{aligned} \tag{24}$$

where $*$ denotes complex conjugate, $0 \ll \lambda < 1$ is the forgetting factor, and $\mu = \beta(1-\lambda)$ is the step-size with $0 < \beta \leq 1$ [16]. It has been found through simulation that this value of μ exhibits stability in terms of convergence for speech signals. Letting σ_x^2 be the input signal variance, the initial regularization parameters [16] are $\mathbf{S}_{\mathrm{MDF}}(0) = \sigma_x^2/100$ and $\delta_{\mathrm{MDF}} = 20\sigma_x^2 N/L$. For a nonstationary signal, σ_x^2 can be estimated in a piecewise manner at each iteration by $\mathbf{x}_s^T(n)\mathbf{x}_s(n)/(2N)$ where $\mathbf{x}_s(n)$ is the first column of the $2N \times 2N$ matrix $\mathbf{C}$. Convergence analysis for the MDF algorithm is provided in [21].

3. THE IPMDF ALGORITHM

3.1. Algorithmic formulation

The proposed IPMDF algorithm exploits both the fast convergence of the improved proportionate normalized least mean square (IPNLMS) algorithm and the efficient implementation of the multidelay adaptive filtering (MDF) algorithm inheriting the beneficial properties of both. We note that direct use of $\mathbf{Q}(n)$, with elements as described by (8), into the weight update equation in (24) is inappropriate since the former is in the time domain whereas the latter is in the frequency domain. Thus our proposed method will be to update the filter coefficients in the time domain. This is achieved by first defining the matrices

$$\begin{aligned}\widetilde{\mathbf{W}}^{\mathbf{10}} &= \left[\mathbf{I}_{N\times N} \quad \mathbf{0}_{N\times N}\right], \\ \widetilde{\mathbf{G}}^{10} &= \widetilde{\mathbf{W}}^{10}\mathbf{F}^{-1}.\end{aligned} \tag{25}$$

We next define, for $k = 0, 1, \ldots, K-1$,

$$\mathbf{q}_k(m) = \left[q_{kN}(m), q_{kN+1}(m), \ldots, q_{kN+N-1}(m)\right] \tag{26}$$

as the partitioned control elements of the kth block such that each element in this block is now determined by

$$q_{kN+j}(m) = \frac{1-\alpha}{2L} + (1+\alpha)\frac{\left|\hat{h}_{kN+j}(m)\right|}{2\|\hat{\mathbf{h}}\|_1 + \epsilon}, \tag{27}$$

where $k = 0, 1, \ldots, K-1$ is the block index while $j = 0, 1, \ldots, N-1$ is the tap-index of each kth block. The IPMDF algorithm update equation is then given by

$$\begin{aligned}\hat{\mathbf{h}}_k(m) = \hat{\mathbf{h}}_k(m-1) &+ L\mu \mathbf{Q}_k(m)\widetilde{\mathbf{G}}^{10}\mathbf{D}^*(m-k) \\ &\times \left[\mathbf{S}_{\mathrm{IPMDF}}(m) + \delta_{\mathrm{IPMDF}}\right]^{-1}\underline{\mathbf{e}}(m),\end{aligned} \tag{28}$$

$$\begin{aligned}
\delta_{\mathrm{IPMDF}} &= \frac{(1-\alpha)\sigma_x^2 20N}{2L} \\
\lambda &= \left[1 - \frac{1}{3L}\right]^N \\
\mu &= \beta(1-\lambda), \quad 0 < \beta \leq 1 \\
\mathbf{S}_{\mathrm{IPMDF}}(0) &= \frac{(1-\alpha)\sigma_x^2}{2\times 100} \\
\hat{\mathbf{h}}(0) &= \mathbf{0}_{L\times 1} \\
\hat{\mathbf{h}}_k(m) &= \left[\hat{h}_{kN}(m), \hat{h}_{kN+1}(m), \ldots, \hat{h}_{kN+N-1}(m)\right]^T \\
j &= 0, 1, \ldots, N-1 \\
q_{kN+j}(m) &= \frac{1-\alpha}{2L} + (1+\alpha)\frac{\left|\hat{h}_{kN+j}(m)\right|}{2\|\hat{\mathbf{h}}\|_1 + \epsilon} \\
\mathbf{q}_k(m) &= \left[q_{kN}(m), q_{kN+1}(m), \ldots, q_{kN+N-1}(m)\right] \\
\mathbf{Q}_k(m) &= \mathrm{diag}\left\{\mathbf{q}_k(m)\right\} \\
\mathbf{G}^{01} &= \mathbf{F}\mathbf{W}^{01}\mathbf{F}^{-1} \\
\widetilde{\mathbf{G}}^{10} &= \widetilde{\mathbf{W}}^{10}\mathbf{F}^{-1} \\
\underline{\hat{\mathbf{h}}}_k(m) &= \mathbf{F}\begin{bmatrix}\hat{\mathbf{h}}_k(m) \\ \mathbf{0}_{N\times 1}\end{bmatrix} \\
\underline{\mathbf{e}}(m) &= \underline{\mathbf{y}}(m) - \mathbf{G}^{01}\sum_{k=0}^{K-1}\mathbf{D}(m-k)\underline{\hat{\mathbf{h}}}_k(m-1) \\
\mathbf{S}_{\mathrm{IPMDF}}(m) &= \lambda \mathbf{S}_{\mathrm{IPMDF}}(m-1) + (1-\lambda)\mathbf{D}^*(m)\mathbf{D}(m) \\
\hat{\mathbf{h}}_k(m) &= \hat{\mathbf{h}}_k(m-1) + L\mu\mathbf{Q}_k(m)\widetilde{\mathbf{G}}^{10}\mathbf{D}^*(m-k) \\
&\quad \times\left[\mathbf{S}_{\mathrm{IPMDF}}(m) + \delta_{\mathrm{IPMDF}}\right]^{-1}\underline{\mathbf{e}}(\mathrm{m}).
\end{aligned}$$

Algorithm 1: The IPMDF algorithm.

where the diagonal control matrix $\mathbf{Q}_k(m) = \mathrm{diag}\{\mathbf{q}_k(m)\}$. The proposed IPMDF algorithm performs updates in the time domain by first computing the gradient of the adaptive algorithm given by $\mathbf{D}^*(m-k)[\mathbf{S}_{\mathrm{IPMDF}}(m) + \delta_{\mathrm{IPMDF}}]^{-1}\underline{\mathbf{e}}(m)$ in the frequency domain. The matrix $\widetilde{\mathbf{G}}^{10}$ then converts this gradient to the time domain so that multiplication with the (time-domain) control matrix $\mathbf{Q}_k(m)$ is possible. The estimated impulse response $\hat{\mathbf{h}}_k(m)$ is then transformed into the frequency domain for error computation given by

$$\underline{\mathbf{e}}(m) = \underline{\mathbf{y}}(m) - \mathbf{G}^{01}\sum_{k=0}^{K-1}\mathbf{D}(m-k)\underline{\hat{\mathbf{h}}}_k(m-1). \tag{29}$$

The IPMDF algorithm can be summarized as shown in Algorithm 1.

3.2. Computational complexity

We consider the computational complexity of the proposed IPMDF algorithm. We note that although the IPMDF algorithm is updated in the time domain, the error $\underline{\mathbf{e}}(m)$ is generated using frequency-domain coefficients and hence five FFT-blocks are required. Since a $2N$ point FFT requires $2N\log_2 N$ real multiplications, the number of multiplications required per output sample for each algorithm is

described by the following relations:

$$\begin{aligned}&\text{IPNLMS: } 4L,\\&\text{FLMS: } 8 + 10\log_2 L,\\&\text{MDF: } 8K + (4K + 6)\log_2 N,\\&\text{IPMDF: } 10K + (4K + 6)\log_2 N.\end{aligned} \tag{30}$$

It can be seen that the complexity of IPMDF is only modestly higher than MDF. However, as we will see in Section 4, the performance of IPMDF far exceeds that of MDF for both speech and white Gaussian noise (WGN) inputs.

4. RESULTS AND DISCUSSIONS

The performance of IPMDF is compared with MDF and IPNLMS in the context of network echo cancellation. This performance can be quantified using the normalized misalignment defined by

$$\eta(m) = \frac{||\mathbf{h} - \hat{\mathbf{h}}(m)||_2^2}{\|\mathbf{h}\|_2^2}, \tag{31}$$

where $\|\cdot\|_2^2$ is defined as the squared l_2-norm operator. Throughout our simulations, we assume that the length of the adaptive filter is equivalent to that of the unknown system. Results are presented over a single trial and the following parameters are chosen for all simulations:

$$\begin{aligned}\alpha &= -0.75,\\ \lambda &= \left[1 - \frac{1}{(3L)}\right]^N,\\ \beta &= 1,\\ \mu &= \beta \times (1 - \lambda),\\ \mathbf{S}_{\text{MDF}}(0) &= \frac{\sigma_x^2}{100},\\ \delta_{\text{MDF}} &= \frac{\sigma_x^2 20N}{L},\\ \mathbf{S}_{\text{IPMDF}}(0) &= \frac{(1-\alpha)\sigma_x^2}{200},\\ \delta_{\text{IPMDF}} &= \frac{20(1-\alpha)\sigma_x^2 N}{(2L)},\\ \delta_{\text{NLMS}} &= \sigma_x^2,\\ \delta_{\text{IPNLMS}} &= \frac{1-\alpha}{2L}\delta_{\text{NLMS}}.\end{aligned} \tag{32}$$

These choices of parameters allow algorithms to converge to the same asymptotic value of $\eta(m)$ for fair comparison.

4.1. Recorded impulse responses

In this first experiment, we investigate the variation of the rate of convergence with frame size N for IPMDF using an impulse response of a 64 milliseconds network hybrid recorded at 8 kHz sampling frequency as shown in Figure 2. Figure 3 shows the convergence with various frame sizes N for IPMDF using a white Gaussian noise (WGN) input sequence. An uncorrelated WGN sequence $w(n)$ is added to achieve a signal-to-noise ratio (SNR) of 30 dB. It can be seen that the convergence is faster for smaller N since the adaptive filter coefficients are being updated more frequently. Additional simulations for $N < 64$ have indicated that no further significant improvement in convergence performance is obtained for lower N values.

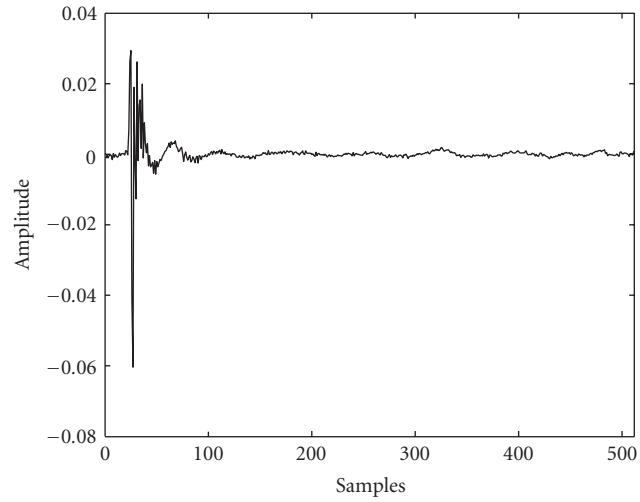

Figure 2: Impulse response of a recorded network hybrid.

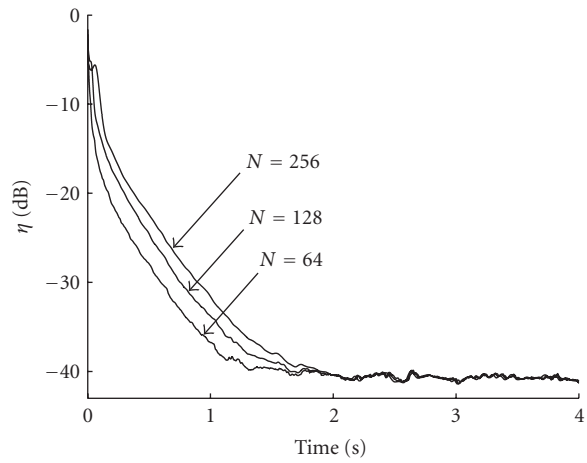

Figure 3: IPMDF convergence for different N with sparse impulse response. SNR = 30 dB.

We compare the relative rate of convergence of the IPMDF, MDF, IPNLMS, and NLMS algorithms using the same impulse response. As before, $w(n)$ is added to achieve an SNR of 30 dB. The frame size for IPMDF and MDF was chosen to be $N = 64$ while the step-size of IPNLMS and NLMS was adjusted so that its final misalignment is the same as that for IPMDF and MDF. This corresponds to $\mu_{\text{IPNLMS}} = \mu_{\text{NLMS}} = 0.15$. Figure 4 shows the convergence for the respective algorithms using a WGN sequence. It can be seen that there is a significant improvement in normalized misalignment of approximately 5 dB during convergence for the IPMDF compared to MDF and IPNLMS.

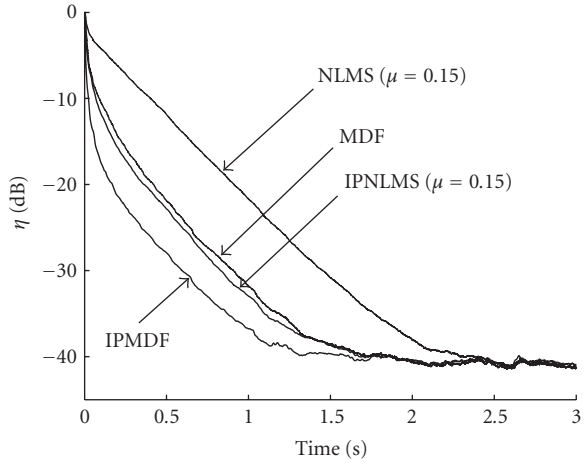

Figure 4: Relative convergence of IPMDF, MDF, IPNLMS, and NLMS using WGN input. SNR = 30 dB.

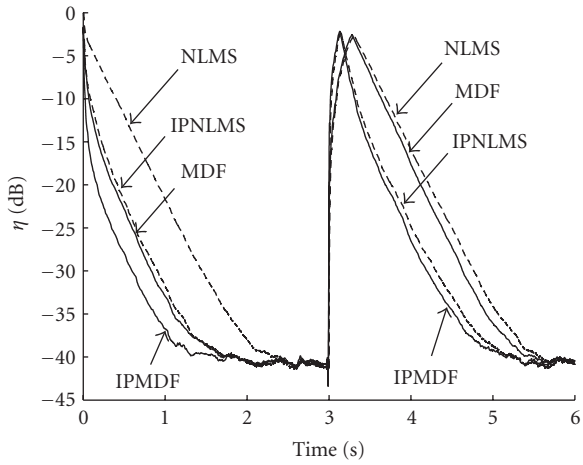

Figure 5: Relative convergence of IPMDF, MDF, IPNLMS, and NLMS using WGN input with echo path change at 3 s. SNR = 30 dB.

We compare the tracking performance of the algorithms as shown in Figure 5 using a WGN input sequence. In this simulation, an echo path change, comprising an additional 12-sample delay, was introduced after 3 seconds. As before, the frame size for the IPMDF and MDF algorithms is $N = 64$ while for IPNLMS and NLMS, $\mu_{\text{IPNLMS}} = \mu_{\text{NLMS}} = 0.15$ is used. We see that IPMDF achieves the highest initial rate of convergence. When compared with MDF, the IPMDF algorithm has a higher tracking capability following the echo path change at 3 seconds. Compared with the IPNLMS algorithm, a delay is introduced by block processing the data input for both the MDF and IPMDF algorithms. As a result, IPNLMS achieves a better tracking capability than the MDF algorithm. The tracking capability of NLMS is slower compared to IPNLMS and IPMDF due to its relatively slow convergence rate. Although delay exists for the IPMDF algorithm, the reduction in delay due to the multidelay structure allows the IPMDF algorithm to achieve an improvement of 2 dB over IPNLMS after echo path change.

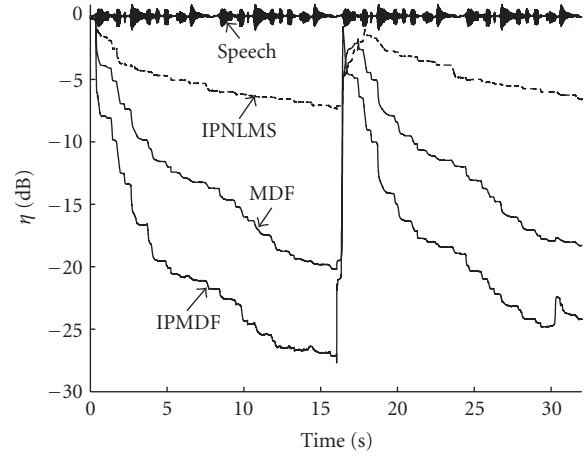

Figure 6: Relative convergence of IPMDF, MDF, and IPNLMS using speech input with echo path change at 3 seconds.

Figure 6 compares the convergence performance of IPNLMS, IPMDF, and MDF using the same experimental setup as before but using a speech input from a male speaker. An echo path change, comprising an additional 12-sample delay, is introduced at 16 seconds. It can be seen that IPMDF achieves approximately 5 dB improvement in normalized misalignment during initial convergence compared to the MDF algorithm.

4.2. Synthetic impulse responses with various degrees of sparseness

We illustrate the robustness of IPMDF to impulse response sparseness. Impulse responses with various degrees of sparseness are generated synthetically using an $L \times 1$ exponentially decaying window [18] which is defined as

$$\mathbf{u} = \left[\mathbf{p}\ 1\ e^{-1/\psi}, e^{-2/\psi}, \ldots, e^{-(L_u-1)/\psi}\right]^T, \tag{33}$$

where the $L_p \times 1$ vector $\mathbf{p}$ models the bulk delay and is a zero mean WGN sequence with variance σ_p^2 and $L_u = L - L_p$ is the length of the decaying window while $\psi \in \mathbb{Z}^+$ is the decay constant. Defining an $L_u \times 1$ vector $\mathbf{b}$ as a zero mean WGN sequence with variance σ_b^2, the $L \times 1$ synthetic impulse response can then be expressed as

$$\mathbf{B} = \text{diag}\{\mathbf{b}\}, \qquad \mathbf{h} = \begin{bmatrix} \mathbf{I}_{L_p \times L_p} & \mathbf{0}_{L_p \times L_u} \\ \mathbf{0}_{L_u \times L_p} & \mathbf{B} \end{bmatrix} \mathbf{u}. \tag{34}$$

The sparseness of an impulse response can be quantified using the sparseness measure [18, 19]

$$\xi(\mathbf{h}) = \frac{L}{L - \sqrt{L}} \left(1 - \frac{\|\mathbf{h}\|_1}{\sqrt{L}\|\mathbf{h}\|_2}\right). \tag{35}$$

It has been shown in [18] that $\xi(\mathbf{h})$ reduces with ψ. Figure 7 shows an illustrative example set of impulse responses generated using (34) with $\sigma_p^2 = 1.055 \times 10^{-4}$, $\sigma_b^2 = 0.9146$,

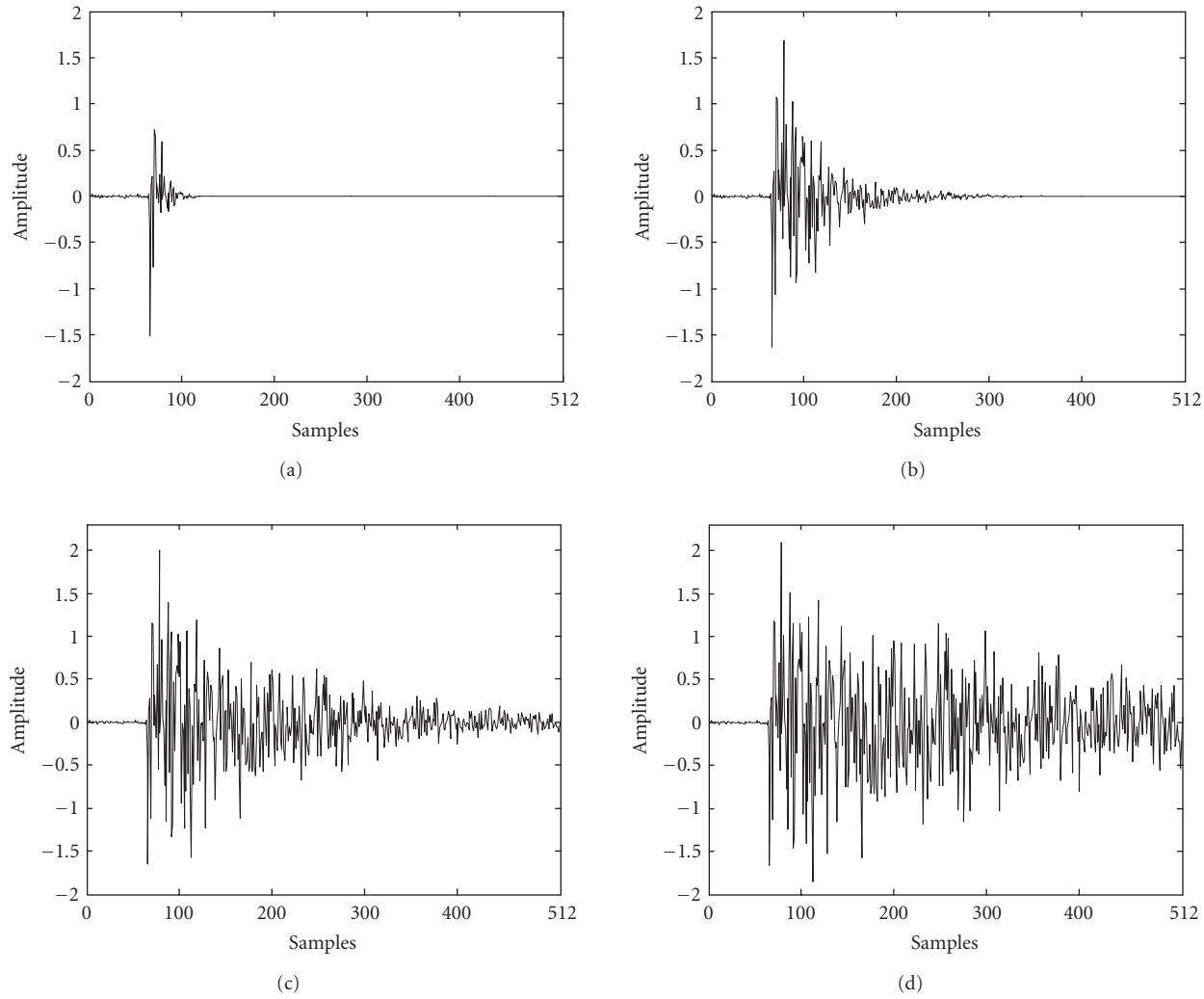

FIGURE 7: Impulse responses controlled using (a) $\psi = 10$, (b) $\psi = 50$, (c) $\psi = 150$, and (d) $\psi = 300$ giving sparseness measure (a) $\xi = 0.8767$, (b) $\xi = 0.6735$, (c) $\xi = 0.4216$, and (d) $\xi = 0.3063$.

$L = 512$, and $L_p = 64$. These impulse responses with various degrees of sparseness were generated using decay constants (a) $\psi = 10$, (b) $\psi = 50$, (c) $\psi = 150$, and (d) $\psi = 300$ giving sparseness measures of (a) $\xi = 0.8767$, (b) $\xi = 0.6735$, (c) $\xi = 0.4216$, and (d) $\xi = 0.3063$, respectively. We now investigate the performance of IPNLMS, MDF, and IPMDF using white Gaussian noise input sequences for impulse responses generated using $0.3 \leq \xi \leq 0.9$ as controlled by ψ. As before $w(n)$ is added to achieve an SNR of 30 dB. Figure 8 shows the variation in time to reach $\eta(m) = -20$ dB normalized misalignment with sparseness measure ξ controlled using exponential window ψ. Due to the proportional control of step-sizes, significant increase in the rate of convergence for IPNLMS and IPMDF can be seen as the sparseness of the impulse responses increases for high ξ. For all cases of sparseness, the IPMDF algorithm exhibits the highest rate of convergence compared to IPNLMS and MDF hence demonstrating the robustness of IPMDF to the sparse nature of the unknown system.

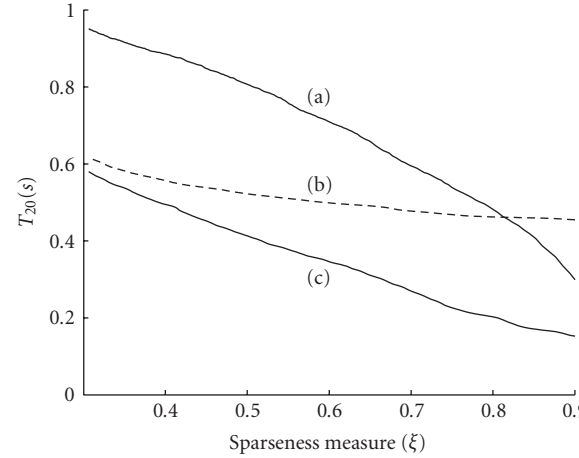

FIGURE 8: Time to reach -20 dB (T_{20}) normalized misalignment for (a) IPNLMS, (b) MDF and (c) IPMDF algorithms with sparseness measure ξ controlled using exponential decay factor ψ.

5. CONCLUSION

We have proposed the IPMDF algorithm for echo cancellation with sparse impulse responses. This algorithm exploits both the improvement in convergence brought about by the proportionality control of IPNLMS and the efficient implementation in the frequency domain of MDF. Simulation results, using both WGN and speech inputs, have shown that the improvement in initial convergence and tracking of IPMDF over MDF for both sparse and dispersive impulse responses far outweighs the modest increase in computational cost.

REFERENCES

[1] J. Radecki, Z. Zilic, and K. Radecka, "Echo cancellation in IP networks," in *Proceedings of the 45th Midwest Symposium on Circuits and Systems*, vol. 2, pp. 219–222, Tulsa, Okla, USA, August 2002.

[2] M. Boujida and J.-M. Boucher, "Higher order statistics applied to wavelet identification of marine seismic signals," in *Proceedings of European Signal Processing Conference (EUSIPCO '96)*, Trieste, Italy, September 1996.

[3] Y.-F. Cheng and D. M. Etter, "Analysis of an adaptive technique for modeling sparse systems," *IEEE Transactions on Acoustics, Speech, and Signal Processing*, vol. 37, no. 2, pp. 254–264, 1989.

[4] E. A. Robinson and T. S. Durrani, *Geophysical Signal Processing*, Prentice-Hall, Englewood Cliffs, NJ, USA, 1986.

[5] D. L. Duttweiler, "Proportionate normalized least-mean-squares adaptation in echo cancelers," *IEEE Transactions on Speech and Audio Processing*, vol. 8, no. 5, pp. 508–518, 2000.

[6] J. Benesty and S. L. Gay, "An improved PNLMS algorithm," in *Proceedings of IEEE International Conference on Acoustics, Speech and Signal Processing (ICASSP '02)*, vol. 2, pp. 1881–1884, Orlando, Fla, USA, May 2002.

[7] J. Cui, P. A. Naylor, and D. T. Brown, "An improved IPNLMS algortihm for echo cancellation in packet-switched networks," in *Proceedings of IEEE International Conference on Acoustics, Speech and Signal Processing (ICASSP '04)*, vol. 4, pp. 141–144, Montreal, Que, Canada, May 2004.

[8] H. Deng and M. Doroslovački, "New sparse adaptive algorithms using partial update," in *Proceedings of IEEE International Conference on Acoustics, Speech and Signal Processing (ICASSP '04)*, vol. 2, pp. 845–848, Montreal, Que, Canada, May 2004.

[9] K. Dogançay and O. Tanrikulu, "Adaptive filtering algorithms with selective partial updates," *IEEE Transactions on Circuits and Systems II: Analog and Digital Signal Processing*, vol. 48, no. 8, pp. 762–769, 2001.

[10] H. Deng and M. Doroslovački, "Improving convergence of the PNLMS algorithm for sparse impulse response identification," *IEEE Signal Processing Letters*, vol. 12, no. 3, pp. 181–184, 2005.

[11] J. W. Cooley and J. W. Tukey, "An algorithm for the machine calculation of complex Fourier series," *Mathematics of Computation*, vol. 19, no. 90, pp. 297–301, 1965.

[12] S. Haykin, *Adaptive Filter Theory*, Information and System Science Series, Prentice-Hall, Englewood Cliffs, NJ, USA, 4th edition, 2002.

[13] J. J. Shynk, "Frequency-domain and multirate adaptive filtering," *IEEE Signal Processing Magazine*, vol. 9, no. 1, pp. 14–37, 1992.

[14] E. Hänsler and G. U. Schmidt, "Hands-free telephones - joint control of echo cancellation and postfiltering," *Signal Processing*, vol. 80, no. 11, pp. 2295–2305, 2000.

[15] J.-S. Soo and K. K. Pang, "Multidelay block frequency domain adaptive filter," *IEEE Transactions on Acoustics, Speech, and Signal Processing*, vol. 38, no. 2, pp. 373–376, 1990.

[16] J. Benesty, T. Gänsler, D. R. Morgan, M. M. Sondhi, and S. L. Gay, *Advances in Network and Acoustic Echo Cancellation*, Springer, New York, NY, USA, 2001.

[17] A. W. H. Khong, J. Benesty, and P. A. Naylor, "An improved proportionate multi-delay block adaptive filter for packet-switched network echo cancellation," in *Proceedings of the 13th European Signal Processing Conference (EUSIPCO '05)*, Antalya, Turkey, September 2005.

[18] J. Benesty, Y. A. Huang, J. Chen, and P. A. Naylor, "Adaptive algorithms for the identification of sparse impulse responses," in *Selected Methods for Acoustic Echo and Noise Control*, E. Hänsler and G. Schmidt, Eds., chapter 5, pp. 125–153, Springer, New York, NY, USA, 2006.

[19] P. O. Hoyer, "Non-negative matrix factorization with sparseness constraints," *Journal of Machine Learning Research*, vol. 5, pp. 1457–1469, 2004.

[20] R. Gray, "On the asymptotic eigenvalue distribution of toeplitz matrices," *IEEE Transactions on Information Theory*, vol. 18, no. 6, pp. 725–730, 1972.

[21] J. Lee and S.-C. Chong, "On the convergence properties of multidelay frequency domain adaptive filter," in *Proceedings of IEEE International Conference on Acoustics, Speech, and Signal Processing (ICASSP '99)*, vol. 4, pp. 1865–1868, Phoenix, Ariz, USA, March 1999.